Continuous versus single H_2O_2 addition in peroxone process: performance improvement and modelling in wastewater effluents

Alberto Cruz-Alcalde*, Santiago Esplugas, Carme Sans

Department of Chemical Engineering and Analytical Chemistry, Faculty of Chemistry, Universitat de Barcelona, C/Martí i Franqués 1, 08028 Barcelona, Spain

*Corresponding author: alberto.cruz@ub.edu

ABSTRACT

Ozonation combined with continuous addition of H_2O_2 was studied as potential strategy for the effective abatement of ozone-resistant micropollutants from wastewater effluents. Oxidant doses within and beyond immediate ozone demand completion were tested. Through experiments involving the continuous addition of H_2O_2 in a semi-continuous contactor, it was demonstrated that this new approach could lead to a 36% reduction of the overall O_3 needs for a constant H_2O_2/O_3 molar ratio of 0.25 compared to single ozonation, representing a 28% reduction in energy consumption. This improvement was mainly attributed to H_2O_2 addition during the secondary ozonation stage, where the direct ozone demand becomes less important. The •OH-exposure per consumed ozone (*i.e.*, R_{OHO3} concept) calculation demonstrated that higher (0.5-1) and lower (0.25) oxidant relationships work better in improving the process performance during initial and secondary stages, respectively. Moreover, continuous versus total initial addition of H_2O_2 were compared and the first one showed better performance, representing differences in

energy costs up to 21%. Finally, two strategies for the real-time control of the O_3-recalcitrant MPs fate were tested, one based on the R_{OHO3} concept and the other on UVA_{254} monitoring. Both resulted in accurate predictions ($R^2 > 0.96$) for different compounds, effluents and processes.

KEYWORDS

O_3/H_2O_2 process, Micropollutants, Oxidant dosing, Process intensification, Kinetic modelling

1. Introduction

Even though ozonation is nowadays stablished as one of the most effective end-of-pipe solutions for micropollutants (MPs) abatement in municipal wastewater effluents [1–5], this process still presents some drawbacks that limit its widespread application. As a consequence of the low reactivity with ozone (O_3) exhibited by some of the MPs typically present in wastewater effluents, as well as the relatively low availability of hydroxyl radicals (•OH) in the system, some of these compounds are not effectively removed when applying this technology [5]. These species are known as ozone-resistant micropollutants, and they typically present second-order rate constants with O_3 lower than 10 $M^{-1}s^{-1}$ [1]. Although current ozone applications do not focus on the complete abatement of these recalcitrant chemicals, water resources stress in some parts of the world may eventually trigger the need for producing high-quality reclaimed wastewater. In this situation, the monitoring and removal of ozone-resistant micropollutants –especially if these represent potential risks to human and environmental health– during ozonation may become

necessary [6–8]. Increasing the oxidant exposure required to effectively remove these species from wastewater effluents would involve the application of larger ozone doses, which can make the process unaffordable, as well as potentially lead to significant generation of harmful oxidation byproducts, such as bromate [9,10]. Combining O_3 with hydrogen peroxide (H_2O_2) can be a practical alternative to improve single ozonation performance while keeping as low as possible the required dose of ozone. By means of this process application, hydroxyl radical (•OH) production is increased with respect to single ozonation, thus allowing larger removals of ozone refractory MPs for equivalent ozone doses [11]. In addition, bromate formation during ozonation of water matrices containing significant amounts of bromide can be significantly reduced in the presence of H_2O_2 [5,12].

A number of previous studies have reported experimental evidence on the benefits –in terms of micropollutants abatement– of employing the O_3/H_2O_2 combination (also known as peroxone process) for drinking water applications [13–15]. However, this enhancement in micropollutants abatement appears to be minimal for water matrices presenting a higher pollution load (*i.e.*, wastewater effluents) [15–17]. Furthermore, interesting aspects of the process –such as the employed H_2O_2 dosing strategy– remain barely explored. In most of the lab-scale studies dealing with the peroxone process, hydrogen peroxide at known H_2O_2/O_3 ratios is dosed before ozone addition from a concentrated ozone stock solution [1,13,16,18]. Similarly, in semi-batch or continuous ozone applications this reagent is added before ozone bubbling or injection [15].

Moreover, the currently employed ozone doses in lab- pilot- and full-scale ozone applications are, in general, not higher than 20 mg L^{-1}. Under these conditions, the

immediate ozone demand (IOD) of secondary effluents is not greatly exceeded, thus limited ozone residual is detected in the reaction medium [19,20]. Therefore, the ozone demand can be considered constant during the whole process and, consequently, there is a single optimal H_2O_2/O_3 ratio for each application. However, as previously stated, the final quality demands for the treated effluent can be more restrictive, requiring the employment of ozone doses beyond IOD completion. In this situation –which would involve a change in the ozone mass transfer regime from gas to liquid phase [20]–, it must be explored if independent H_2O_2/O_3 ratios during each one of the two stages of the process could be required in order to optimize the overall process performance in terms of oxidation efficiency.

Another aspect of the peroxone process that requires to be further investigated in its application is the monitoring and control of ozone-resistant micropollutants abatement. In most related works, a prediction based in the use of the time-integrated concentration of hydroxyl radicals in the reaction medium (*i.e.*, the hydroxyl radical exposure $\int[\bullet OH]\,dt$) has proven to be feasible and accurate [17,21,22]. However, this term needs to be previously calculated by means of experiments involving the use of a probe compound [23], fact that hinders the full-scale application of this control strategy for real-time monitoring. In this sense, the use of easily measurable parameters such as the transferred ozone dose (TOD) or the evolution of ultraviolet absorbance at 254 nm (UVA_{254}) as surrogates for hydroxyl radical exposure could be a practical option. Recently, it has been shown that these two parameters were highly correlated during single ozonation process [24,25]. Thus, they could also be helpful for the kinetic modelling of peroxone process with simultaneous O_3 and H_2O_2 addition.

In summary, this work aimed to evaluate the use of simultaneous ozone and hydrogen peroxide addition as new strategy in peroxone process applied for the enhancement of ozone-resistant micropollutants abatement in a semi-batch ozone contactor. The main objective was describing the process performance in terms of oxidation efficiency under different operational conditions (*i.e.*, H_2O_2/O_3 ratios), stablishing comparisons between continuous (*i.e.*, simultaneous to ozone bubbling) and initial (*i.e.*, before ozone bubbling) addition of H_2O_2. The concluding objective was testing practical modelling strategies potentially allowing the real-time monitoring and control of ozone-resistant MPs removal during this process application.

2. Materials and methods

2.1. Chemicals and reagents

N-[(6-chloro-3-pyridyl)methyl]-*N'*-cyano-*N*-methyl-acetamidine (acetamiprid, ACMP) , 6-chloro-*N*2-ethyl-*N*4-(propan-2-yl)-1,3,5-triazine-2,4-diamine (atrazine, ATZ) and 2-(4-(2-methylpropyl)phenyl)propanoic acid (ibuprofen, IBU) analytical standards were acquired from Sigma-Aldrich (Germany). Ammonium vanadate (V) (99.0%) was supplied by Fluka. Ultrapure water was produced by a filtration system (Millipore, USA). Pure oxygen (≥ 99.999%) for ozone production was supplied by Abelló Linde (Spain). The rest of reagents, including hydrogen peroxide solution (30% w/v), were acquired from Panreac (Spain).

2.2. Wastewater effluents

Three wastewater effluents were collected from WWTPs in the Metropolitan Area of Barcelona (Spain) were employed in this work. Two of them (MBR-1, MBR-2) came from membrane biological reactor (MBR) systems, whereas sample CAS-3 was collected from the secondary settler after a conventional activated sludge (CAS) unit. Their quality parameters are summarized in Table 1. All samples were refrigerated at 4 ºC until use.

Table 1. Effluent quality parameters. All measurements were carried out per triplicate, being discrepancies between obtained values lower than 5% in all cases.

WWTP ID	**Location**	**pH**	**TOC [mg C L^{-1}]**	**DOC [mg C L^{-1}]**	**UVA_{254} [m^{-1}]**	**Turbidity [NTU]**	**Alkalinity [mg $CaCO_3$ L^{-1}]**	**NO_2^- [mg N L^{-1}]**
MBR-1	Vallvidrera	7.8	7.2	7.1	0.091	0.3	448.1	0.03
MBR-2	Gavà-Viladecans	7.7	13.6	13.3	0.174	0.5	208.3	0.19
CAS-3	Gavà-Viladecans	7.8	51.1	21.7	0.503	18.5	469.4	0.16

Main differences in water quality presented by effluents were, in summary: the relative content in both, organic and inorganic carbon (the latter expressed as alkalinity) and the presence of solid and colloidal matter of the CAS-3 sample, compared with the MBR effluents. These marked variations in water properties were expected to illustrate the matrix effect on the process performance for a wide range of effluent qualities.

2.3. Ozonation of wastewater effluents

Ozonation experiments were performed in a semi-continuous, jacketed contactor with a working volume of 750 mL. Ozone was produced by a 301.19 lab ozonizer (Sander,

145 Germany) and injected at the bottom of the reactor by means of a fritted glass diffuser
146 (pore size: 150-250 µm). A proper contact between gas and liquid phases was ensured by
147 means of a mechanical mixing system. Experiments were performed at a temperature of
148 20±1 ºC, without pH adjustment. The gas flow rate and the inlet ozone concentration were
149 set at 0.1 NL min^{-1} and 30 mg NL^{-1}, respectively. The ozone concentrations at the inlet
150 and the outlet gas streams were continuously measured by means of two BMT 964 ozone
151 analyzers (BMT Messtechnik, Germany). A Q45H/64 dissolved O_3 probe (Analytical
152 Technology, USA) was placed in a liquid recirculation stream (flow rate: 0.2 L min^{-1}) and
153 allowed the measurement of the ozone concentration in the reaction medium. A detailed
154 scheme of the ozonation setup can be found elsewhere [24].
155
156 Ozone consumption at each reaction time was determined as the transferred ozone dose
157 (TOD), which represents the accumulated amount of ozone that is transferred to the water
158 sample per unit of volume and time, according to Eq. 1. F_g, V_{liq} stand for, respectively,
159 the gas flow and the volume of the liquid phase; t is the contact time; and $[O_3]_{in}$ and
160 $[O_3]_{out}$ represent the inlet and outlet ozone concentrations in the gas phase, respectively.
161

$$TOD = \int_0^t \frac{F_g}{V_{liq}} \cdot ([O_3]_{in} - [O_3]_{out}) \cdot \mathrm{d}t \quad (1)$$

162
163 Each wastewater effluent was spiked with 100 µg L^{-1} of ACMP, which was employed as
164 •OH probe compound according to the methodology explained in detail by Elovitz and
165 von Gunten and based on the use of an ozone-resistant compound to that purpose [23].
166 Then, the solution was homogenized by the mechanical stirring prior to the treatment.
167 Subsequently, the wastewater was ozonized for 60 min under the operational conditions

168 before described. Samples withdrawn at specific reaction times were analyzed for ACMP
169 and H_2O_2 residuals, as well as for UV absorbance at 254 nm when required.
170
171 Additional experiments were performed in order to illustrate the usefulness of R_{OHO3}
172 concept in the prediction of ozone-recalcitrant micropollutants removal during peroxone
173 process application. In this case, the pesticide atrazine (ATZ) and the drug ibuprofen
174 (IBU) were selected because both are typical ozone-resistant compounds. Thus, each
175 wastewater effluent was spiked with low concentrations (50 µg L^{-1}) of ATZ and IBU.
176
177 MPs, including ACMP, ATZ and IBU are typically found in wastewater effluents at
178 concentrations not higher than the µg/L level. Being so, we selected these concentrations
179 (100 µg/L for ACMP and 50 µg/L for ATZ and IBU) because they did not represent a
180 high oxidant scavenging during the process and allowed us to monitor their residual
181 concentrations by HPLC-DAD.
182
183 *2.4. Hydrogen peroxide dosing*
184
185 During O_3/H_2O_2 experiments, hydrogen peroxide addition was performed by means of
186 two different methods: a) continuous dosing through a metering pump; or b) direct spiking
187 from the commercial solution, before ozone injection. For O_3/H_2O_2 experiments with
188 continuous hydrogen peroxide dosing, an Ismatec 829 metering pump (Cole-Parmer,
189 Germany) connecting the contactor and a reservoir tank containing the H_2O_2 solution was
190 employed. The flow-rate was set at the lowest possible value (0.33 mL min^{-1}) to minimize
191 the medium dilution. In order to apply H_2O_2/O_3 molar ratios of 0.25, 0.5 and 1 when
192 working in continuous dosing mode, the transferred ozone dose per unit time (TOD/t, mg

193 O_3 L^{-1} min^{-1}) was employed as reference for H_2O_2 addition. As ozonation typically
194 exhibits a two-stage –one fast, one slow– behavior regarding the ozone transfer to the
195 liquid phase [20], two TOD/t values determined in single ozonation experiments were
196 employed as reference in each experiment to calculate the H_2O_2 flow-rate required to
197 meet the working H_2O_2/O_3 ratios during the whole treatment. Two fresh H_2O_2 solutions
198 –one per process stage– were prepared just before starting the peroxone experiments
199 (concentrations of stock solutions included in Table S1 in the Supplementary
200 Information). Hydrogen peroxide was initially supplied from the first solution –more
201 concentrated, due to a faster ozone consumption at the beginning of the process–, until
202 the characteristic transition between fast and slow ozone transfer regimes was reached.
203 From this point, and until the end of the experiment, H_2O_2 was pumped from the second
204 –and more diluted– stock solution. In experiments with initial H_2O_2 dosing, a dose
205 equivalent to the total amount of peroxide added in continuous addition experiments was
206 transferred to the reaction medium shortly before ozone bubbling. Details regarding
207 particular dosing conditions for all the experiments performed are gathered in Section 3.2
208 (Table 2).
209
210 *2.5. Analytical procedures*
211
212 Total organic carbon (TOC) and dissolved organic carbon (DOC, previous filtration
213 through 0.45 µm PTFE filters) were determined by means of a TOC-VCSN analyzer
214 (Shimadzu, Japan). UVA_{254} was measured by means of a DR6000 spectrophotometer
215 (Hach, USA). Turbidity was determined by means of a 2100Q turbidimeter (Hach, USA).
216 Alkalinity was measured employing an automatic titrator (Hach, Spain). Nitrite (NO_2^-)
217 concentration was measured by ion-exchange chromatography with UV detection. H_2O_2

residual concentration was determined through the vanadate (V) spectrophotometric procedure [26]. The concentrations of ACMP, ATZ and IBU were quantified by means of a high performance liquid chromatograph (HPLC) equipped with a diode array detector (DAD), all supplied by Agilent (1260 Infinity). The column employed was a Teknokroma Mediterranea Sea18 (250 mm x 4.6 mm and 5µm size packing). The flow rate and injection volume were set, respectively, at 1.0 mL min^{-1} and 100 µL in all determinations. For ACMP analyses, the mobile phase consisted of 30:70 volumetric mixtures of acetonitrile and Milli-Q water acidified at pH 3 by the addition of H_3PO_4. The detection wavelength was set to 250 nm. For ATZ and IBU quantification, the mobile phase consisted of 70:30 volumetric mixtures of acetonitrile and pH 3 Milli-Q water, and the UV detection was performed at 225 nm. The limits of quantitation were 3.3 µg L^{-1}, 0.9 µg L^{-1} and 2.1 µg L^{-1} for ACMP, ATZ and IBU, respectively.

3. Results and discussion

3.1. Fate of ACMP as a model O_3-resistant compound during wastewater single ozonation

Fig. 1 shows the evolution of ACMP as a function of the TOD in single ozonation experiments extended to ozone doses up to 60 mg L^{-1}. ACMP is a neonicotinoid pesticide which barely reacts with ozone (k_{O3} = 0.25 $M^{-1}s^{-1}$) and presents a high second-order rate constant for its reaction with hydroxyl radicals ($k_{\bullet OH}$) of $2.1 \cdot 10^9$ $M^{-1}s^{-1}$ [27]. Because of these properties, this chemical was selected in the present study as model ozone-recalcitrant micropollutant. In the view of the obtained ACMP degradation profiles, typically employed ozone doses (according to multiple lab-, pilot- and full-scale studies

found in literature, ranging from 5 to 20 mg L^{-1}), represented by a shaded area in Fig. 1, do not provide enough •OH-exposure to achieve important removal levels for this compound (between 20% and 40% depending on the effluent). Similar conclusions can be drawn from results reported over the last years in ozonation studies focused in the abatement of selected micropollutants that also included in their list some compounds with low ozone reactivity [1,2,4,13,28]. However, the ozone doses required to achieve acceptable degradation levels (*e.g.*, > 80%) for these species were insufficiently discussed in those reports, probably because ozonation of wastewater effluents was not extended beyond typically employed O_3 dosages. For the three wastewater effluents, and depending on their different contents in organic matter and alkalinity (that is, the water matrix components considered to be mainly responsible for •OH scavenging during ozonation [5]) the applied doses to achieve an 80% degradation level should be 37 mg L^{-1}, 43 mg L^{-1} and 51 mg L^{-1} for MBR-1, MBR-2 and CAS-3, respectively. This represents an increment, compared to the considered maximum dose of 20 mg L^{-1}, between 46% and 61%. Another interesting information drawn from these results is the fact that the IOD (represented in Fig. 1 by dashed lines) needs to be completed –and indeed significantly exceeded– in order to reach the transferred ozone doses required for O_3-recalcitrant MPs abatement.

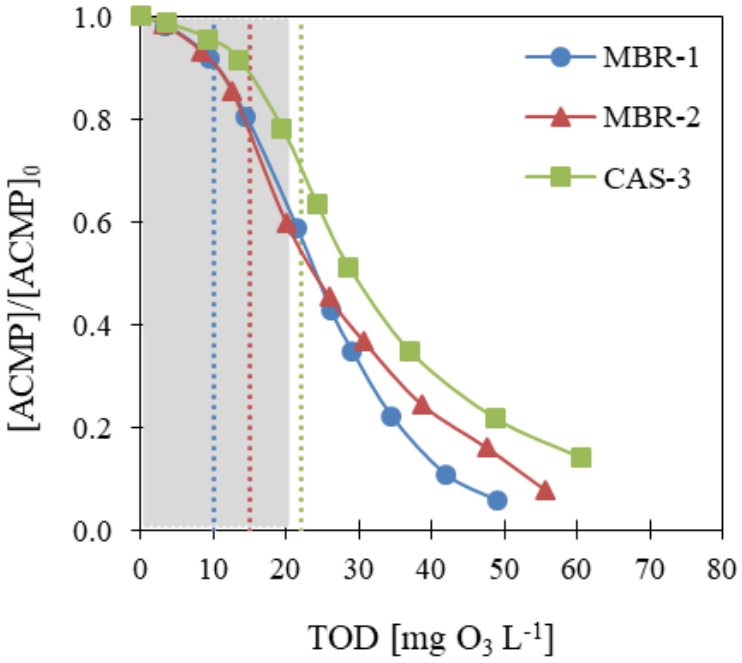

Figure 1. Removal of ACMP from wastewater effluents by means of single ozonation: C/C_0 profiles versus TOD. The shaded area indicates the currently applied range of O_3 doses in full- pilot- and lab scale applications, and the dashed lines represent the IOD values of the tested effluents. Experimental conditions: $[ACMP]_0$: 100 µg L^{-1}; F_g: 0.1 NL min^{-1}; $[O_3]_{in}$: 30 mg NL^{-1}; T: 20 ºC.

Fig. S1 (see the Supplementary Information) illustrate changes taking place in the ozone transfer efficiencies during single ozonation experiments extended up to transferred ozone doses (TOD) of 60 mg L^{-1}. Approximately after IOD completion –which according to the results obtained took place for TOD values between 10 mg L^{-1} and 22 mg O_3 L^{-1}, depending on the water source (see Fig. S1, right column plots) – the ozone transfer efficiency from gaseous to liquid phase notably decreases (before IOD, η_{tr1}: 0.69-0.74; after IOD, η_{tr2}: 0.12-0.19). This two-stage behavior in ozone transfer is a consequence of two different O_3 demands exerted by the water matrix components at different oxidation extents [20]. As above mentioned, if ozone demand is different during the two regimes of the process, the optimal H_2O_2/O_3 ratios to enhance the •OH production are expected to vary from primary to secondary ozonation stages. This is explored in the next section.

3.2. *Peroxone with H_2O_2 continuous addition for enhanced abatement of ozone-recalcitrant ACMP*

Peroxone process extended beyond IOD with continuous H_2O_2 addition were conducted in semi-batch ozonation mode. Table 2 gathers particular H_2O_2 dosing conditions for each one of the experiments carried out. First, the process is described in terms of oxidation performance and then comparisons between continuous or initial addition of hydrogen peroxide are presented. In experiments with initial H_2O_2 addition, the dose of this oxidant was selected according to the total H_2O_2 dose in continuous addition experiments (Table 2, last column).

Table 2. Hydrogen peroxide dosing conditions during peroxone experiments. Total H_2O_2 dose values presented in the last column represent the total amount of hydrogen peroxide dosed in continuous addition experiments, and also the dose of this reagent applied in experiments with total initial addition.

Effluent	**H_2O_2/O_3 ratio (molar)**	**H_2O_2 dose, Stage 1 [mg L^{-1}]**	**H_2O_2 dose, Stage 2 [mg L^{-1}]**	**Total H_2O_2 dose [mg L^{-1}]**
MBR-1	0	-	-	-
	0.25	4.00	8.15	12.15
	0.5	6.95	17.35	24.30
	1	14.65	33.95	48.60
MBR-2	0	-	-	-
	0.25	3.97	8.38	12.35
	0.5	6.95	17.74	24.69
	1	14.35	35.03	49.38

	0	-	-	-
CAS-3	0.25	3.81	11.05	14.86
	0.5	7.28	22.50	29.78
	1	17.52	42.00	59.52

294

295 *3.2.1. Removal of ACMP at different H_2O_2/O_3 ratios: process efficiency*

296

297 Although peroxone process has proven to be effective for enhanced •OH production from
298 O_3 decomposition, some studies dealing with the use of this combination in wastewater
299 effluents have reported that only a little improvement in O_3-resistant MPs abatement is
300 observed, compared to single ozonation [15–17]. All previous works were performed
301 with total H_2O_2 addition at the beginning of the ozonation process. Fig. 2 (left column)
302 show ACMP degradation profiles during continuous hydrogen peroxide dosage in
303 peroxone application in wastewater effluents MBR-1, MBR-2 and CAS-3 at different
304 H_2O_2/O_3 constant ratios. As it can be observed, addition of hydrogen peroxide improves
305 the overall degradation efficiency, even at the lowest employed H_2O_2/O_3 ratio (*i.e.*, 0.25).
306 For that particular condition, ozone doses required to eliminate 80% of the initial ACMP
307 were reduced from 37 mg L^{-1} to 24 mg L^{-1} for MBR-1, from 43 mg L^{-1} to 26 mg L^{-1} for
308 MBR-2 and from 51 mg L^{-1} to 34 mg L^{-1} for CAS-3. Those changes represent a 36%
309 decrease in the overall O_3 needs. Of course, the use of hydrogen peroxide involves
310 additional costs that need to be considered when performing the corresponding economic
311 assessment. However, if we consider typical energy costs of 15 kWh/kg and 10 kWh/kg
312 for O_3 and H_2O_2 production [18], respectively, the overall energy consumption is reduced
313 in this particular case by 28%, pointing out the global benefit of peroxone process on
314 recalcitrant micropollutant removal in municipal effluents. This is in contrast with
315 previous results from literature in which the power consumption was incremented by 25%

316 [18]. This, however, can be attributed to the fact that ozone was always dosed at sub-IOD
317 concentrations, that is, when O_3 demand exerted by the water matrix was high. In this
318 situation, ozone is very unstable and its decomposition in water is controlled by radical-
319 type chain reactions with effluent organic matter (EfOM) [5]. In addition, •OH generation
320 may be hindered by ozone reactions not conducting to hydroxyl radical formation (e.g.,
321 reaction between O_3 and nitrite [29]).
322

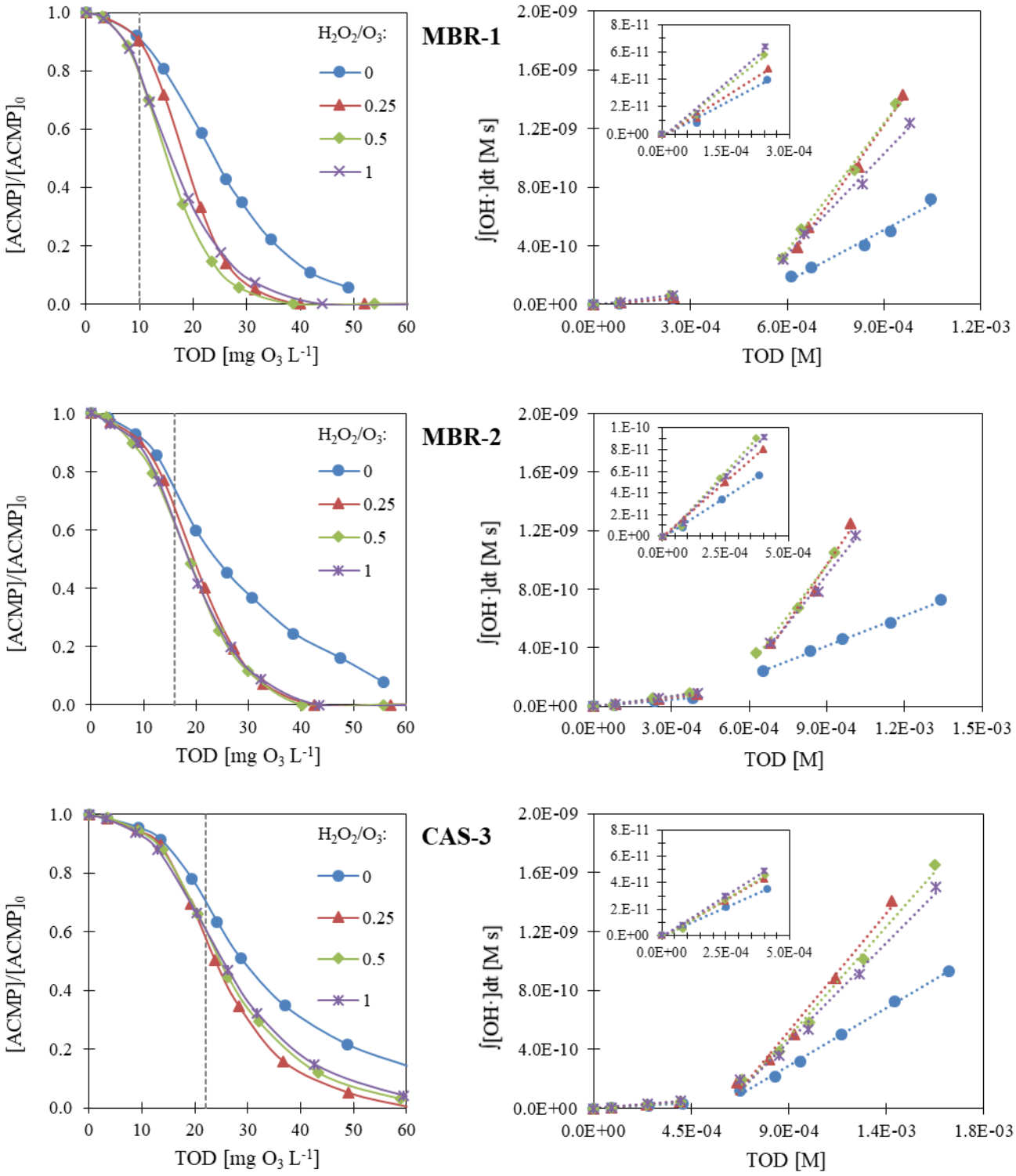

Figure 2. Removal of ACMP by O_3 and O_3/H_2O_2 processes from effluents MBR-1, MBR-2 and CAS-3 with continuous H_2O_2 addition at different oxidant ratios (left column); and ∫[•OH]dt vs TOD plot for each experiment (right column). Dashed lines in the first plot indicate the IOD values. Insets in the latter are a zoom of the plot region corresponding to the initial reaction stage. Experimental conditions: $[ACMP]_0$: 100 µg L^{-1}; F_g: 0.1 NL min^{-1}; $[O_3]_{in}$: 30 mg NL^{-1}; T: 20 ºC.

From the degradation profiles of ACMP, it is clear that the effect of continuous H_2O_2 addition on the oxidation efficiency becomes more significant after IOD completion. During the initial (or IOD) stage, the ozone decay process is mainly controlled by O_3 reactions with EfOM, and little enhancement in the pesticide removal is observed. However, during the secondary stage (*i.e.*, after IOD has been satisfied), more O_3 is available to react with the deprotonated form of hydrogen peroxide (HO_2^-), leading to an enhancement in •OH production compared to single ozonation. That is the main reason why the improved oxidation of the model compound was mostly observed during the second stage of the process.

The mechanisms explaining hydroxyl radical generation in peroxone are well described by Eqs. gathered in Table 3. Most of these reactions are common to the mechanism of ozone decay initiated by the hydroxide anion (Eq. 2), although this initiation step is markedly slower than the peroxone reaction (Eq. 5). In fact, the contribution of hydroxide-initiated mechanisms to ozone decomposition in wastewater ozonation is typically insignificant, and O_3 decay is mainly driven by reactions with other matrix constituents such as EfOM [5]. In the peroxone process, on the contrary, the higher reaction kinetics can, to some extent, compete with the main O_3 decay reactions and give rise to •OH generation with a yield of 0.5 [30].

Table 3. Ozone decomposition mechanisms initiated by the hydroxide (OH^-) and hydroperoxide (HO_2^-) anions.

Reaction	**Rate constants**	**Reaction No.**	**References**
$O_3 + OH^- \rightarrow HO_4^-$	$k_2 = 70\ M^{-1}s^{-1}$	(2)	[31–33]

$HO_4^- \leftrightarrow HO_2^\bullet + O_2^{\bullet-}$	$k_3 \sim 10^7\ s^{-1}$	(3)	[31]
	$k_{-3} = 5 \cdot 10^9\ M^{-1}s^{-1}$		
$HO_2^\bullet + O_2^{\bullet-} \rightarrow HO_2^- + O_2$	$k_4 = 10^8\ M^{-1}s^{-1}$	(4)	[31]
$O_3 + HO_2^- \rightarrow HO_5^-$	$k_5 = 2.8 \cdot 10^6\ M^{-1}s^{-1}$	(5)	[32,34]
$HO_5^- \leftrightarrow HO_2^\bullet + O_3^{\bullet-}$	$k_6 > 10^7\ s^{-1}$	(6)	[34]
	$k_{-6} \sim 5 \cdot 10^9\ M^{-1}s^{-1}$		
$HO_5^- \rightarrow 2O_2 + OH^-$	$k_7 \sim k_5$	(7)	[34]
$HO_2^\bullet \leftrightarrow O_2^{\bullet-} + H^+$	$k_8 = 3.2 \cdot 10^5\ s^{-1}$	(8)	[32]
	$k_{-8} = 2.0 \cdot 10^{10}\ M^{-1}s^{-1}$		
$O_3 + O_2^{\bullet-} \rightarrow O_3^{\bullet-} + O_2$	$k_9 = 1.6 \cdot 10^9\ M^{-1}s^{-1}$	(9)	[35]
$O_3^{\bullet-} \leftrightarrow O^{\bullet-} + O_2$	$k_{10} = 1.94 \cdot 10^3\ s^{-1}$	(10)	[34]
	$k_{-10} = 3.5 \cdot 10^9\ M^{-1}s^{-1}$		
$O^{\bullet-} + H_2O \leftrightarrow HO^\bullet + OH^-$	$k_{11} = 9.6 \cdot 10^7\ s^{-1}$	(11)	[31,36]
	$k_{-11} = 1.2 \cdot 10^{10}\ M^{-1}s^{-1}$		
$HO^\bullet + O_3 \rightarrow O_2 + HO_2^\bullet$	$k_{12} = 2.0 \cdot 10^9\ M^{-1}s^{-1}$	(12)	[33]
$H_2O_2 + {}^\bullet OH \rightarrow HO_2^\bullet + H_2O$	$k_{13} = 2.7 \cdot 10^7\ M^{-1}s^{-1}$	(13)	[5]

In addition, carbonate radicals ($CO_3^{\bullet-}$) usually formed during the O_3/H_2O_2 treatment are expected to promote ozone decomposition (Eq. 14, [37]) to finally yield hydroxyl radicals by some of the aforementioned mechanisms. This effect may become more significant during the second stage of the process, as selective $CO_3^{\bullet-}$ reactivity with EfOM –which contributes to the inhibition of ozone decomposition (Eq. 15, [38])– may be lower after IOD completion [39–41].

$$CO_3^{\bullet-} + H_2O_2 \rightarrow HCO_3^- + HO_2^\bullet \quad (14)$$

$$CO_3^{\bullet-} + EfOM \leftrightarrow CO_3^{2-} + products \quad (15)$$

Variations between effluents or operational conditions in the peroxone process performance, in terms of oxidation efficiency, can be well reflected by the R_{OHO3} concept. This parameter is calculated as the •OH-exposure per consumed ozone [42] and represents a recent alternative to related parameters established decades ago for performance characterization of ozone-based processes. In fact, it is a modified version of both the oxidation-competition value (Ω_M) and the R_{ct} concept –introduced by Hoigné and Bader [43] and Elovitz and von Gunten [23], respectively– which according to experimental evidences overcomes some limitations presented by these classical parameters [42]. In the present work, the R_{OHO3} value has been calculated according to Eq. 16.

$$R_{OHO_3} = \frac{\int [\bullet OH]\, dt}{TOD} \quad (16)$$

Fig. 2 (right column) show the R_{OHO3} plots for each wastewater. Data fitted well a two-stage linear model, each one of these stages corresponding to the two ozone transfer regimes observed during the process. For the initial stage, characterized by a strong oxidant demand, R_{OHO3} values were between $0.11 \cdot 10^{-6}$ s and $0.39 \cdot 10^{-6}$ s for different wastewaters and experimental conditions (*i.e.*, H_2O_2/O_3 ratios). After IOD, however, significantly larger values (between $0.96 \cdot 10^{-6}$ s and $4.2 \cdot 10^{-6}$ s) were registered. Like single ozonation processes, differences observed between effluents can be attributed to water properties, mainly organic matter content and alkalinity. Both components, organic species and carbonates, exert a scavenging effect over hydroxyl radicals that reduces their availability in the reaction medium and decreases the MPs oxidation efficiency. Detailed

explanations regarding the influence of these parameters in the value of R_{OHO3} during ozonation can be found elsewhere [24,42].

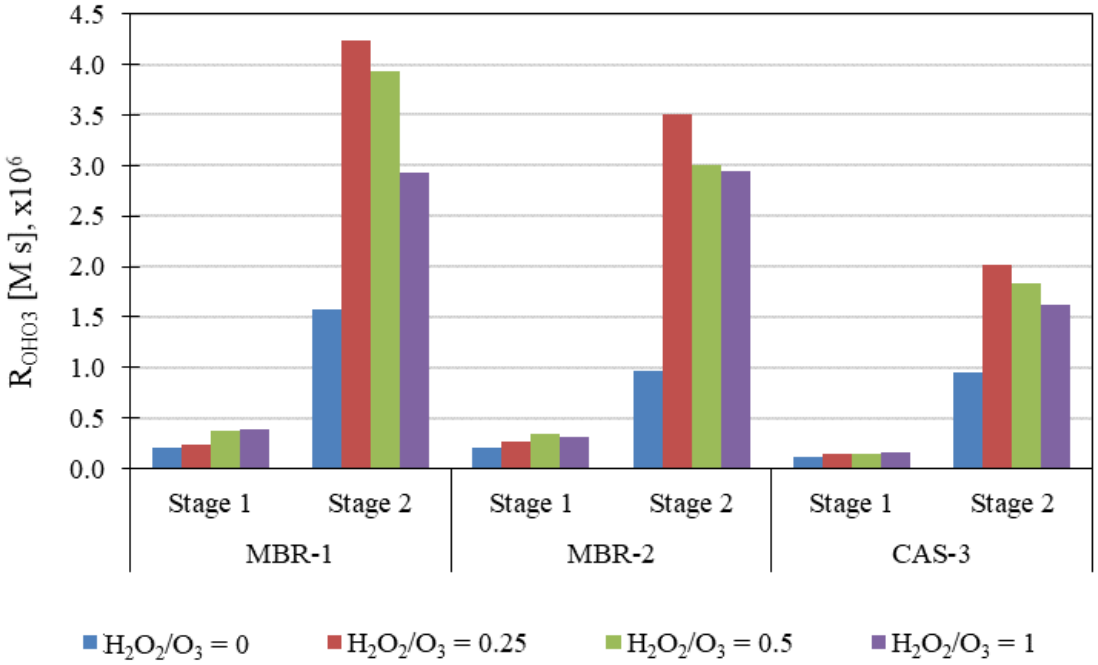

Figure 3. Comparison of R_{OHO3} values obtained from ACMP degradation experiments from effluents MBR-1, MBR-2 and CAS-3 employing O_3 and the combination O_3/H_2O_2 at different oxidant ratios (data represented in Fig. 1), before (Stage 1) and after (Stage 2) IOD. Experimental conditions: $[ACMP]_0$: 100 µg L^{-1}; F_g: 0.1 NL min^{-1}; $[O_3]_{in}$: 30 mg NL^{-1}; T: 20 ºC.

The R_{OHO3} concept can be also useful to investigate the optimal conditions (*i.e.*, H_2O_2/O_3 ratios) for extended peroxone application with continuous H_2O_2 addition. Fig. 3 shows the R_{OHO3} variation for effluents MBR-1, MBR-2 and CAS-3 at different H_2O_2/O_3 ratios, before (Stage 1) and after (Stage 2) IOD. One can readily notice that the effect of H_2O_2 addition is much more significant after the IOD, as already advanced in view of the ACMP degradation profiles. On the contrary, the oxidation efficiency during the initial stage of the process is little afected. The above mentioned differences in the scale of values from initial to secondary regimes are also noticed in the view of this graph. It is

399 also interesting here the observed fact that for all three effluents, regardless of their water
400 properties, the H_2O_2/O_3 ratios showing best performances for pre- and post-IOD stages
401 are different. Larger relationships (and therefore, larger amounts of H_2O_2) are required
402 during the initial stage of the process, compared to the post-IOD phase. Concretely,
403 H_2O_2/O_3 ratios between 0.5 and 1 showed better perfomances for initial process stage,
404 whereas for post-IOD step the best oxidant relationship was 0.25. This fact may be
405 attributed to the strong O_3 demand exerted by the water matrix during the initial steps of
406 the treatment, which control the ozone decomposition process. In this situation, higher
407 H_2O_2/O_3 ratios are required if some enhancing effect by H_2O_2 (*i.e.*, •OH-exposure
408 increase) is wanted to be observed. On the contrary, after IOD completion the oxidant
409 demand exerted by the water matrix is much lower, which allows a larger ozone
410 availability in the reaction medium compared to the first stage. Therefore, the amount of
411 hydrogen peroxide required to initiate ozone decomposition to •OH is also lower. Dosing
412 H_2O_2 during the second stage at H_2O_2/O_3 ratios larger than 0.25 appeared to conduct to a
413 decrease in the oxidation efficiency for all three effluents, as observed in Fig. 3. Although
414 differences are not very large, these can be most probably attributed to •OH scavenging
415 by hydrogen peroxide accumulated after IOD completion (see Table S2). In fact, only
416 limited consumption of H_2O_2 (11-23% of the total) took place during the initial ozonation
417 stage, whereas most of it (*i.e.*, 77-89% of the total) was consumed during the second stage
418 of the process. Although other components of wastewater such as EfOM and
419 carbonate/bicarbonate typically contribute more to hydroxyl radical scavenging than
420 H_2O_2 [5], the scavenging capacity of the water matrix could have been altered after TOD
421 values of 10, 16 and 22 mg O_3 L^{-1} (consumed by effluents MBR-1, MBR-2 and CAS-3,
422 respectively). This, together with the mentioned accumulation of hydrogen peroxide

during IOD completion, therefore constitute the most logical explanation to the modest, although significant, observed decreases in the treatment efficiency.

From the above results, the optimal point to start the addition of hydrogen peroxide during the ozonation process for an improvement on ozone recalcitrant MP removal appears to be after IOD completion. The scarce enhancement in the model compound removal observed at the initial stage, especially compared with the good performance observed once IOD is completed, constitutes a strong argument to make this decision. Moreover, ozone doses applied at the initial stage are relatively low, and this oxidant is instantaneously consumed by high organic and inorganic compounds content during that period. Therefore, the potential formation of significant amounts of bromate is an unlikely risk. Nevertheless, this last statement should be experimentally corroborated.

3.2.2. Continuous versus initial H_2O_2 dosing

During the application of extended peroxone process, and according to the results presented so far in this work, it seems clear that two different H_2O_2/O_3 ratios individually optimized for each one of the process stages should be employed if the best possible overall treatment performance is wanted to be achieved. In order to further prove the necessity of optimizing the H_2O_2 addition strategy, continuous versus initial dosing of H_2O_2 was compared in additional experiments. Fig. 4 (a-c) shows ACMP degradation profiles for peroxone experiments applied to effluents MBR-1, MBR-2 and CAS-3 at a H_2O_2/O_3 ratio of 0.25 and continuous or initial hydrogen peroxide dosing. In Fig. 4d, R_{OHO3} variations corresponding to those experiments are also represented. As it can be seen, the overall process efficiency for all effluents was better when operating with

448 continuous peroxide addition. These differences, however, were more significant in the
449 case of experiments with effluents MBR-1 and MBR-2. In those cases, the addition of
450 H_2O_2 in continuous and initial mode resulted in mean decreases of the ozone requirements
451 to abate ACMP by 80% of 37% and 18 %, respectively, compared to single ozonation
452 process. These reductions in the ozone dose correspond to overall energy savings of
453 around 30% and 9%, respectively. The potential benefits of continuous H_2O_2
454 implementation instead of total initial dosing, therefore, become evident in the view of
455 these data. On the other hand, overall differences observed in the oxidation performance
456 when employing one or other operational modes were less obvious in the case of effluent
457 CAS-3. For that particular scenario, the reduction in the O_3 needs only represented an
458 extra 5% of energy savings when comparing continuous to initial addition (26% vs 21%,
459 respectively).
460

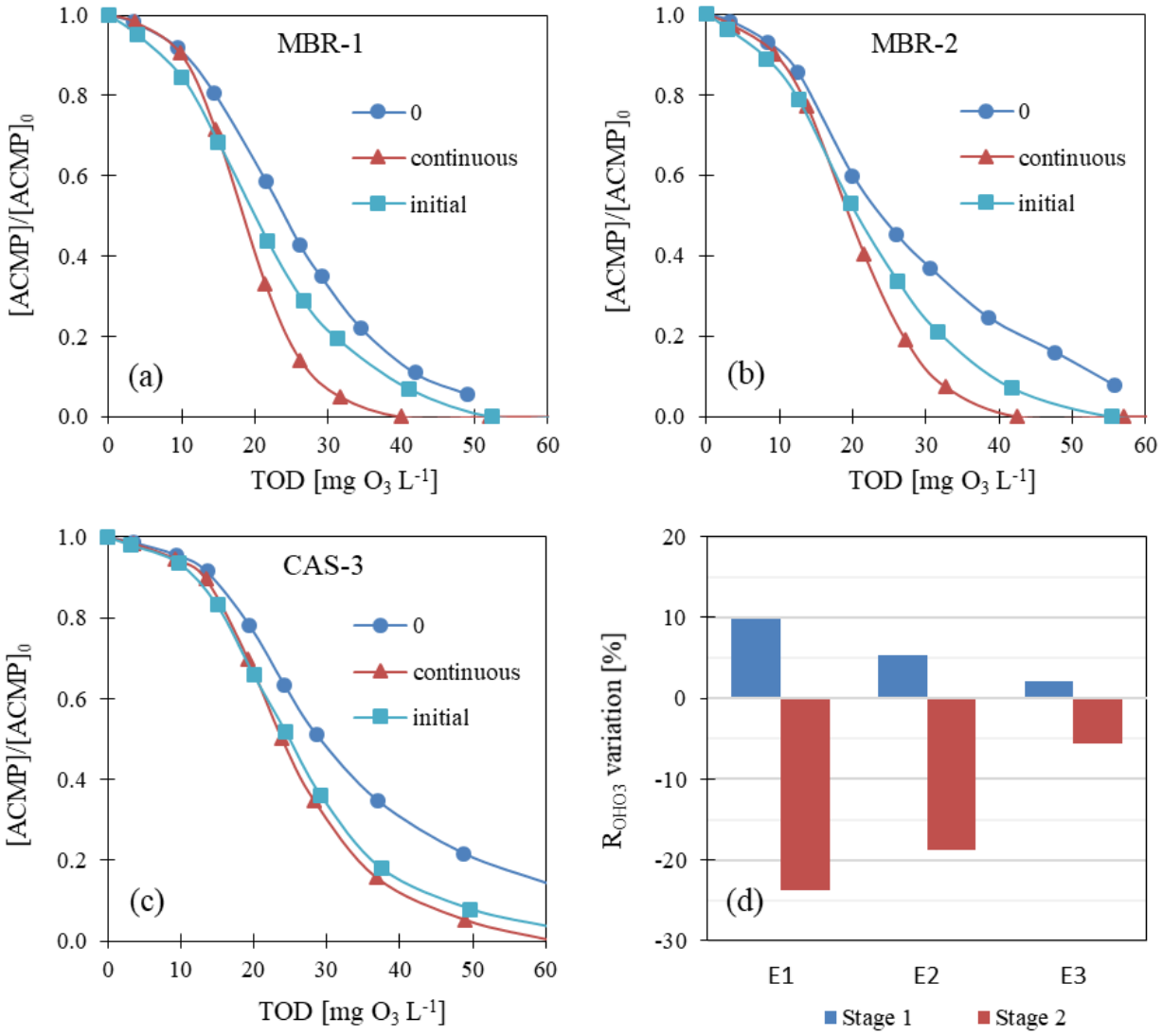

Figure 4. Removal of ACMP from effluents MBR-1, MBR-2 and CAS-3 by O_3 and O_3/H_2O_2 combination: comparison between continuous and initial addition of H_2O_2 (H_2O_2/O_3 ratio = 0.25). Figs. a) - c): ACMP evolution with TOD; Fig. d): R_{OHO3} percent variation for experiments with initial addition compared to experiments with continuous dosing. Experimental conditions: $[ACMP]_0$: 100 µg L^{-1}; F_g: 0.1 NL min^{-1}; $[O_3]_{in}$: 30 mg NL^{-1}; T: 20 ºC.

According to Figure 4, it seems that the excess of hydrogen peroxide at the beginning of the reaction in experiments with initial H_2O_2 addition slightly favored the process performance during its first stage, but negatively affected it –compared to experiments with continuous dosing of H_2O_2– after IOD completion. Similarly to the observed decrease of the treatment efficiency observed in experiments with simultaneous addition

of both oxidants, hydroxyl radical scavenging by an excess of H_2O_2 is most probably the main explanation to these findings.

Overall, H_2O_2 initial addition compared to simultaneous oxidant application resulted in a clearly lower performance of ACMP oxidation. The initial enhancement followed by a decrease in the oxidation efficiency was more evident for the cleanest waters (*i.e.*, MBR-1 and MBR-2), as illustrated in Figs. 4(a-c) and especially in Fig. 4d. The latter clearly show how the R_{OHO3} parameter, which indicates the •OH availability per ozone dose, is between 2 and 10% higher during the initial stage of experiments with initial H_2O_2 addition compared with experiments carried out with continuous dosing. The contrary happened during stage 2, for which this value was significantly lower (up to 24%, depending on the effluent) compared to continuous addition experiments.

It is important to mention that the reduction in the overall O_3 needs required for ACMP oxidation observed in continuous versus initial H_2O_2 experiments at a H_2O_2/O_3 ratio of 0.25 was also noticed in experiments performed at larger H_2O_2/O_3 relationships (*i.e.*, 0.5 and 1). These results can be found in the SI (Fig. S2). Differences in the O_3 savings observed when comparing continuous to initial addition slightly increased for the particular case of effluent CAS-3 to 8% and 12% for H_2O_2/O_3 ratios of 0.5 and 1, respectively. However, these extra savings, compared to the one obtained with a H_2O_2/O_3 ratio of 0.25, would probably not justify the application of higher amounts of hydrogen peroxide, which would increase the absolute costs of the treatment.

In the view of the results presented in this section, adding hydrogen peroxide simultaneously to ozone could be useful to maximize the oxidation efficiency during the

peroxone process application. This novel strategy also involves the change of H_2O_2 dosing between the primary and secondary stages of the process, or even the decission of starting the addition of this reagent once IOD has been completed, as H_2O_2 dosing at the first stage does not contribute in a significant way to the overall improvement of ozone-recalcitrant micropollutant depletion.

3.3. Monitoring of O_3-resistant micropollutants removal

For a reliable, cost-effective real-time monitoring and control of the fate of O_3-recalcitrant MPs during the application of O_3 and O_3/H_2O_2 processes, it may be necessary the use of surrogate parameters whose evolution along the treatment is closely correlated with the abatement of these species. Moreover, the continuous measurement of the selected surrogate along the wastewater treatment should be technically feasible in order to represent a potentially implementable option in full-scale applications. In this sense, the use of UVA_{254} seems to be one of the most practical choices [25,44–47]. In previous studies, it has been experimentally demonstrated how the decay of this parameter can be well correlated to hydroxyl radical exposure (see [24,25] and Eq. 17) when applying single ozonation process to wastewater effluents. However, the potential use of this prediction strategy during the application of peroxone process has not been explored yet. As an example, Fig. 5 shows the natural logarithm of UVA_{254} residual versus hydroxyl radical exposure for O_3/H_2O_2 experiments with effluent MBR-1 and continuous addition of hydrogen peroxide. Data obtained for effluents MBR-2 and CAS-3 can be found in the SI (Fig. S3). Linear correlation coefficients (R^2) higher than 0.95 were obtained in all cases. In accordance with results, two different linear regressions were observed for each experiment, corresponding to the fast and slow kinetic regimes of the process. Since

hydrogen peroxide can absorb radiation at 254 nm [48], residual H_2O_2 concentrations measured during peroxone experiments with initial peroxide addition should be taken into account for potential corrections. However, the poor molar absorptivity of this oxidant and the relatively low residual concentrations detected during experiments with continuous addition of H_2O_2 resulted in minor impacts on $\int[\bullet OH]dt$-UVA_{254} correlations. Thus, data without further corrections was employed this time.

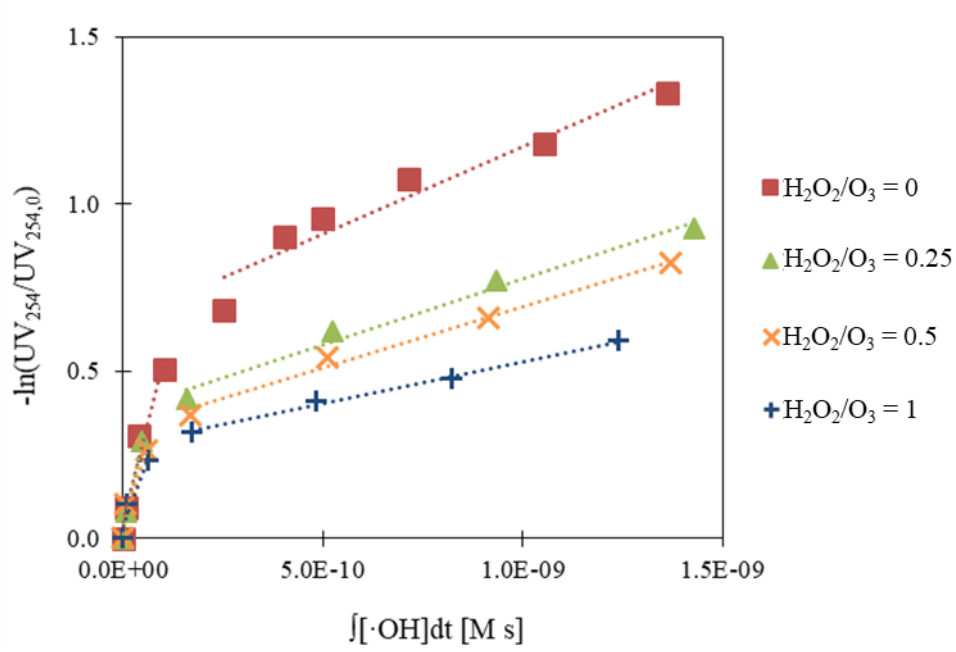

Figure 5. Correlation between UVA_{254} abatement and hydroxyl radical exposure during continuous H_2O_2 addition peroxone experiments with effluent MBR-1 and different H_2O_2/O_3 ratios. Experimental conditions: $[ACMP]_0$: 100 µg L^{-1}; F_g: 0.1 NL min^{-1}; $[O_3]_{in}$: 30 mg NL^{-1}; T: 20 ºC.

Predictions in •OH-exposure based on the use of UVA_{254} monitoring (Eq. 17) allow the estimation of O_3-resistant MPs abatement, according to second-order kinetics (Eq. 18, [5]). In addition, the R_{OHO3} concept (Eq. 16) can be used to estimate the $\int[\bullet OH]dt$ term if the TOD is known at any time interval, which was the case of the present work.

$$-ln\left(\frac{UVA_{254}}{UVA_{254,0}}\right) = k_{UVA,OH} \cdot \int [\bullet OH]\, dt \quad (17)$$

$$-ln\left(\frac{[MP]}{[MP]_0}\right) = k_{\bullet OH} \int [\bullet OH]\, dt \quad (18)$$

Fig. 6 shows predicted and experimental data obtained for single ozonation and peroxone experiments (continuous peroxide addition and H_2O_2/O_3 ratios of 0.25) in the studied effluents regarding the abatement during this process of two typical O_3-resistant micropollutants: the drug ibuprofen (IBU, k_{O3}: 9.6 $M^{-1}s^{-1}$ and $k_{\bullet OH}$: $7.4 \cdot 10^9$ $M^{-1}s^{-1}$ [49]) and the pesticide atrazine (ATZ, k_{O3}: 6.0 $M^{-1}s^{-1}$ and $k_{\bullet OH}$: $3.0 \cdot 10^9$ $M^{-1}s^{-1}$ [21]). The predicted fate of these chemicals during the process was estimated by means of both UVA_{254}- and R_{OHO3}-based models. Good agreements between model predictions and measured data was observed in all cases (R^2 of 0.97 and 0.96 for data predicted through R_{OHO3}- and UVA_{254}-based models, respectively), with apparent independence from effluents, oxidation processes or micropollutants employed.

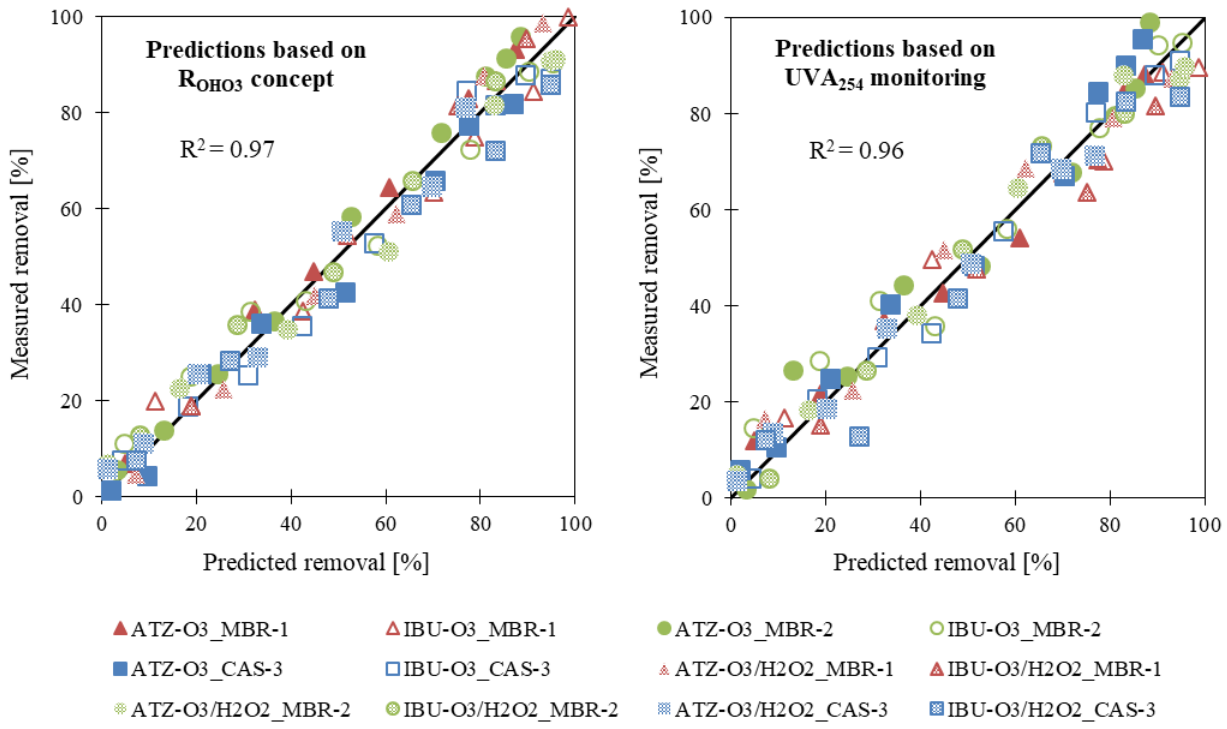

Figure 6. Measured versus predicted removals for atrazine and ibuprofen in effluents MBR-1, MBR-2 and CAS-3 in single ozonation and peroxone experiments (H_2O_2/O_3 ratio = 0.25, continuous addition). Predictions were performed employing two different models: one based on the R_{OHO3} concept (left figure) and the other on the existing correlation between •OH-exposure and the UVA_{254} decay during the treatment. Experimental conditions: $[ACMP]_0$: 100 µg L^{-1}; F_g: 0.1 NL min^{-1}; $[O_3]_{in}$: 30 mg NL^{-1}; T: 20 ºC.

Conclusions

This work demonstrates that the optimization of the H_2O_2 addition strategy is essential to improve the oxidation performance of peroxone process. Continuous dosing of H_2O_2 during ozonation significantly enhanced both •OH availability and MP abatement, for all studied wastewaters. Larger relationships (from 0.5 to 1) worked better during the initial or IOD stage, whereas H_2O_2/O_3 ratio of 0.25 was optimal during the secondary ozonation stage. By following this strategy, overall ozone needs could be reduced by 36% (employed H_2O_2/O_3 ratio: 0.25) with respect to single ozonation, which approximately corresponded to 28% savings in the overall energy costs associated to oxidants use. In

addition, continuous H_2O_2 dosing was demonstrated to perform better than total initial addition of this reagent, estimating energy requirements to be up to 21% lower in the first case and for the cleanest effluents. The observed improvement in the oxidation efficiency, however, was generally little during the initial stage and became especially important after IOD. This work also demonstrated that UV absorbance of the water matrix, as surrogate for •OH-exposure estimation, can be used to control the fate of organic species with low ozone reactivity. This strategy has proven to be useful for the accurate abatement prediction of different O_3-recalcitrant MPs from water matrices presenting a wide range of quality, employing single ozonation or the peroxone process as oxidative treatment.

Acknowledgements

This work was financially supported by the Spanish Ministry of Economy and Competitiveness (project CTQ2017-86466-R and Alberto Cruz's FPI fellowship BES-2015-074109) and the Agency for Management of University and Research Grants of the Government of Catalonia (project 2017SGR131).

References

[1]Y. Lee, D. Gerrity, M. Lee, A.E. Bogeat, E. Salhi, S. Gamage, R.A. Trenholm, E.C. Wert, S.A. Snyder, U. von Gunten, Prediction of micropollutant elimination during ozonation of municipal wastewater effluents: Use of kinetic and water specific information, Environ. Sci. Technol. 47 (2013) 5872–5881. doi:10.1021/es400781r.

[2]Y. Schindler Wildhaber, H. Mestankova, M. Schärer, K. Schirmer, E. Salhi, U. von Gunten, Novel test procedure to evaluate the treatability of wastewater with ozone,

595 Water Res. 75 (2015) 324–335. doi:10.1016/j.watres.2015.02.030.
596 [3]J. Gomes, R. Costa, R.M. Quinta-Ferreira, R.C. Martins, Application of ozonation for
597 pharmaceuticals and personal care products removal from water, Sci. Total
598 Environ. 586 (2017) 265–283. doi:10.1016/J.SCITOTENV.2017.01.216.
599 [4]M. Bourgin, B. Beck, M. Boehler, E. Borowska, J. Fleiner, E. Salhi, R. Teichler, U.
600 von Gunten, H. Siegrist, C.S. McArdell, Evaluation of a full-scale wastewater
601 treatment plant upgraded with ozonation and biological post-treatments:
602 Abatement of micropollutants, formation of transformation products and oxidation
603 by-products, Water Res. 129 (2018) 486–498.
604 doi:10.1016/J.WATRES.2017.10.036.
605 [5]C. von Sonntag, U. von Gunten, Chemistry of Ozone in Water and Wastewater
606 Treatment: From Basic Principles to Applications, IWA Publishing, 2012.
607 [6]D. Fatta-Kassinos, D.D. Dionysiou, K. Kümmerer, Wastewater Reuse and Current
608 Challenges, Springer, 2016.
609 [7]W.W.A. Programme, The United Nations World Water Development Report 2015:
610 Water for a Sustainable World, Paris, 2015.
611 [8]D. Bixio, C. Thoeye, J. De Koning, D. Joksimovic, D. Savic, T. Wintgens, T. Melin,
612 Wastewater reuse in Europe, Desalination. 187 (2006) 89–101.
613 doi:10.1016/J.DESAL.2005.04.070.
614 [9]E.C. Wert, F.L. Rosario-Ortiz, D.D. Drury, S.A. Snyder, Formation of oxidation
615 byproducts from ozonation of wastewater, Water Res. 41 (2007) 1481–1490.
616 doi:10.1016/j.watres.2007.01.020.
617 [10] U. Von Gunten, Ozonation of drinking water: Part II. Disinfection and by-product
618 formation in presence of bromide, iodide or chlorine, Water Res. 37 (2003) 1469–
619 1487. doi:10.1016/S0043-1354(02)00458-X.

620 [11] J.L. Acero, U. von Gunten, Characterization of oxidation processes: ozonation and
621 the AOP O3/H2O2, Am. Water Work. Assoc. 93 (2001) 90–100.
622 [12] U. von Gunten, Y. Oliveras, Kinetics of the reaction between hydrogen peroxide
623 and hypobromous acid: implication on water treatment and natural systems, Water
624 Res. 31 (1997) 900–906.
625 [13] H. Wang, J. Zhan, W. Yao, B. Wang, S. Deng, J. Huang, G. Yu, Y. Wang,
626 Comparison of pharmaceutical abatement in various water matrices by
627 conventional ozonation, peroxone (O3/H2O2), and an electro-peroxone process,
628 Water Res. 130 (2018) 127–138. doi:10.1016/j.watres.2017.11.054.
629 [14] M. Bourgin, E. Borowska, J. Helbing, J. Hollender, H.-P. Kaiser, C. Kienle, C.S.
630 McArdell, E. Simon, U. von Gunten, Effect of operational and water quality
631 parameters on conventional ozonation and the advanced oxidation process
632 O3/H2O2: Kinetics of micropollutant abatement, transformation product and
633 bromate formation in a surface water, Water Res. 122 (2017) 234–245.
634 doi:10.1016/j.watres.2017.05.018.
635 [15] A.N. Pisarenko, B.D. Stanford, D. Yan, D. Gerrity, S.A. Snyder, Effects of ozone
636 and ozone/peroxide on trace organic contaminants and NDMA in drinking water
637 and water reuse applications, Water Res. 46 (2012) 316–326.
638 doi:10.1016/j.watres.2011.10.021.
639 [16] U. Hübner, I. Zucker, M. Jekel, Options and limitations of hydrogen peroxide
640 addition to enhance radical formation during ozonation of secondary effluents, J.
641 Water Reuse Desalin. 5 (2015) 8. doi:10.2166/wrd.2014.036.
642 [17] Y. Lee, D. Gerrity, M. Lee, A.E. Bogeat, E. Salhi, S. Gamage, R.A. Trenholm,
643 E.C. Wert, S.A. Snyder, U. von Gunten, Prediction of micropollutant elimination
644 during ozonation of municipal wastewater effluents: Use of kinetic and water

specific information, Environ. Sci. Technol. 47 (2013) 5872–5881. doi:10.1021/es400781r.

[18] I.A. Katsoyiannis, S. Canonica, U. von Gunten, Efficiency and energy requirements for the transformation of organic micropollutants by ozone, O3/H2O2and UV/H2O2, Water Res. 45 (2011) 3811–3822. doi:10.1016/j.watres.2011.04.038.

[19] M. Roustan, H. Debellefontaine, Z. Do-Quang, J.-P. Duguet, Development of a Method for the Determination of Ozone Demand of a Water, Ozone Sci. Eng. 20 (1998) 513–520. doi:10.1080/01919519809480338.

[20] M. Marce, B. Domenjoud, S. Esplugas, S. Baig, Ozonation treatment of urban primary and biotreated wastewaters: Impacts and modeling, Chem. Eng. J. 283 (2016) 768–777. doi:10.1016/j.cej.2015.07.073.

[21] J.L. Acero, K. Stemmler, U. von Gunten, Degradation kinetics of atrazine and its degradation products with ozone and OH radicals: A predictive tool for drinking water treatment, Environ. Sci. Technol. 34 (2000) 591–597. doi:10.1021/es990724e.

[22] Y. Lee, U. Von Gunten, Advances in predicting organic contaminant abatement during ozonation of municipal wastewater effluent: Reaction kinetics, transformation products, and changes of biological effects, Environ. Sci. Water Res. Technol. 2 (2016) 421–442. doi:10.1039/c6ew00025h.

[23] M.S. Elovitz, U. von Gunten, Hydroxyl Radical/Ozone Ratios During Ozonation Processes. I. The Rct Concept, Ozone Sci. Eng. 21 (1999) 239–260. doi:10.1080/01919519908547239.

[24] A. Cruz-Alcalde, S. Esplugas, C. Sans, Abatement of ozone-recalcitrant micropollutants during municipal wastewater ozonation: kinetic modelling and

surrogate-based control strategies, Chem. Eng. J. (2018). doi:10.1016/j.cej.2018.10.206.

[25] M. Chys, W.T.M. Audenaert, E. Deniere, S.T.F.C. Mortier, H. Van Langenhove, I. Nopens, K. Demeestere, S.W.H. Van Hulle, Surrogate-Based Correlation Models in View of Real-Time Control of Ozonation of Secondary Treated Municipal Wastewater—Model Development and Dynamic Validation, Environ. Sci. Technol. 51 (2017) 14233–14243. doi:10.1021/acs.est.7b04905.

[26] R.F.P. Nogueira, M.C. Oliveira, W.C. Paterlini, Simple and fast spectrophotometric determination of H2O2in photo-Fenton reactions using metavanadate, Talanta. 66 (2005) 86–91. doi:10.1016/j.talanta.2004.10.001.

[27] A. Cruz-Alcalde, C. Sans, S. Esplugas, Priority pesticides abatement by advanced water technologies: The case of acetamiprid removal by ozonation, Sci. Total Environ. 599–600 (2017) 1454–1461. doi:10.1016/j.scitotenv.2017.05.065.

[28] Y. Lee, L. Kovalova, C.S. McArdell, U. von Gunten, Prediction of micropollutant elimination during ozonation of a hospital wastewater effluent, Water Res. 64 (2014) 134–148. doi:10.1016/j.watres.2014.06.027.

[29] S. Naumov, G. Mark, A. Jarocki, C. von Sonntag, The Reactions of Nitrite Ion with Ozone in Aqueous Solution – New Experimental Data and Quantum-Chemical Considerations, Ozone Sci. Eng. 32 (2010) 430–434. doi:10.1080/01919512.2010.522960.

[30] A. Fischbacher, T.C. Schmidt, The • OH Radical Yield in the H 2 O 2 + O 3 (Peroxone) Reaction, Environ. Sci. Technol. 47 (2013) 9959–9964. doi:10.1021/es402305r.

[31] G. Merényi, J. Lind, S. Naumov, C. von Sonntag, The Reaction of Ozone with the Hydroxide Ion : Mechanistic Considerations Based on Thermokinetic and

695 Quantum Chemical Calculations and the Role of HO4- in Superoxide Dismutation,
696 Chem. a Eur. J. 16 (2010) 1372–1377. doi:10.1002/chem.200802539.
697 [32] J. Staehelln, J. Hoigné, Decomposition of Ozone in Water : Rate of Initiation by
698 Hydroxide Ions and Hydrogen Peroxide, (1982) 676–681.
699 doi:10.1021/es00104a009.
700 [33] J. Staehelin, R.E. Buhler, J. Hoigné, Ozone Decomposition In Water Studied by
701 Pulse Radiolysis. 2. OH and HO4 as Chain Intermediates, J. Phys. Chem. 88 (1984)
702 5999–6004. doi:10.1021/j150668a051.
703 [34] G. Merényi, J. Lind, S. Naumov, C. von Sonntag, Reaction of Ozone with
704 Hydrogen Peroxide (Peroxone Process): A Revision of Current Mechanistic
705 Concepts Based on Thermokinetic and Quantum-Chemical Considerations,
706 Environ. Sci. Technol. 44 (2010) 3505–3507. doi:10.1021/es100277d.
707 [35] R.E. Buhler, J. Staehelin, J. Hoigné, Ozone Decompositlon in Water Studied by
708 Pulse Radiolysis. 1. HO2/O2- and HO3/O3- as Intermediates, J. Phys. Chem. 88
709 (1984) 2560–2564. doi:10.1021/j150656a026.
710 [36] G.A. Poskrebyshev, P. Neta, R.E. Huie, Temperature Dependence of the Acid
711 Dissociation Constant of the Hydroxyl Radical, J. Phys. Chem. A. 106 (2002)
712 11488–11491. doi:10.1021/jp020239x.
713 [37] Z.D. Draganić, A. Negrón-Mendoza, K. Sehested, S.I. Vujošević, R. Navarro-
714 Gonzáles, M.G. Albarrán-Sanchez, I.G. Draganić, Radiolysis of aqueous solutions
715 of ammonium bicarbonate over a large dose range, Int. J. Radiat. Appl.
716 Instrumentation. Part. 38 (1991) 317–321. doi:10.1016/1359-0197(91)90100-G.
717 [38] P. Westerhoff, R. Song, G. Amy, R. Minear, Applications of ozone decomposition
718 models, Ozone Sci. Eng. 19 (1997) 55–73. doi:10.1080/01919519708547318.
719 [39] P. Neta, R.E. Huie, A.B. Ross, Rate constants for reactions of inorganic radicals in

720 aqueous solution, J.Phys.Chem.Ref.Data. 17 (1988) 1027–1284.
721 [40] C. Wu, K.G. Linden, Phototransformation of selected organophosphorus
722 pesticides: Roles of hydroxyl and carbonate radicals, Water Res. 44 (2010) 3585–
723 3594. doi:10.1016/j.watres.2010.04.011.
724 [41] S. Canonica, T. Kohn, M. Mac, F.J. Real, J. Wirz, U. Von Gunten, Photosensitizer
725 method to determine rate constants for the reaction of carbonate radical with
726 organic compounds, Environ. Sci. Technol. 39 (2005) 9182–9188.
727 doi:10.1021/es051236b.
728 [42] M. Kwon, H. Kye, Y. Jung, Y. Yoon, J.-W. Kang, Performance characterization
729 and kinetic modeling of ozonation using a new method: ROH,O3 concept, Water
730 Res. (2017). doi:10.1016/j.watres.2017.05.062.
731 [43] J. Hoigné, H. Bader, "Oxidation- Competition Values" of Different Types of
732 Waters Used in Switzerland, Ozone Sci. Eng. 1 (1979) 357–372.
733 doi:10.1080/01919512.1979.10684571.
734 [44] M. Stapf, U. Miehe, M. Jekel, Application of online UV absorption measurements
735 for ozone process control in secondary effluent with variable nitrite concentration,
736 Water Res. 104 (2016) 111–118. doi:10.1016/j.watres.2016.08.010.
737 [45] M. Park, T. Anumol, K.D. Daniels, S. Wu, A.D. Ziska, S.A. Snyder, Predicting
738 trace organic compound attenuation by ozone oxidation: Development of indicator
739 and surrogate models, Water Res. 119 (2017) 21–32.
740 doi:10.1016/j.watres.2017.04.024.
741 [46] G. V Korshin, Evolution of Absorbance Spectra of Ozonated Wastewater and Its
742 Relationship with the Degradation of Trace-Level Organic Species, 44 (2010)
743 6130–6137.
744 [47] E.C. Wert, F.L. Rosario-Ortiz, S.A. Snyder, Using ultraviolet absorbance and color

745 to assess pharmaceutical oxidation during ozonation of wastewater, Environ. Sci.
746 Technol. 43 (2009) 4858–4863. doi:10.1021/es803524a.
747 [48] K.E. O'Shea, D.D. Dionysiou, Advanced Oxidation Processes for Water
748 Treatment, 2018. doi:10.1021/jz300929x.
749 [49] M.M. Huber, S. Canonica, G.Y. Park, U. von Gunten, Oxidation of
750 pharmaceuticals during ozonation and advanced oxidation processes, Environ. Sci.
751 Technol. 37 (2003) 1016–1024. doi:10.1021/es025896h.
752